Clay Minerals (2021), **56**, 65–74
doi:10.1180/clm.2021.17

CAMBRIDGE UNIVERSITY PRESS

Article

Synthesis of Fe-layered double hydroxide from bittern and its nitrate-ion removal ability

Takaaki Wajima*
Graduate School of Engineering, Chiba University, 1-33 Yayoi-cho, Inage-ku, Chiba 263-8522, Japan

Abstract

Nitrate contamination of surface waters and groundwater is one of the main problems associated with agricultural activities worldwide, and there is an urgent need to develop effective materials and processes to remove efficiently excess nitrate from aquatic environments. Bittern is a seawater resource that contains large amounts of Mg^{2+} and Ca^{2+}, and its utilization has received much recent attention. In this study, an Fe-type layered double hydroxide (Fe-LDH) product was prepared from bittern with the addition of an inexpensive agent ($FeCl_3$) for nitrate removal. The greatest nitrate removal was obtained for synthesis conditions of pH 8.5–9.5 at 50°C for 0.5 h. The equilibrium adsorption capacity of the product for nitrate was measured and fitted with the Langmuir and Freundlich isotherm models. The experimental data better fit the Langmuir model than the Freundlich model. The calculated maximum adsorption capacity for nitrate was 0.40 mmol g^{-1}, which was greater than those of other reported nitrate adsorbents. The product removed nitrate ions from a highly saline solution. The order of interference of anion species for nitrate removal was $CO_3^{2-} > SO_4^{2-} > Br^- > NO_2^- > Cl^- > F^-$. The pH of the solution and removal of nitrate increased with increasing solution temperature because of ion exchange between the Cl^- in Fe-LDH and the NO_3^- in the solution. Nitrate ions were repeatedly adsorbed and desorbed. The prepared Fe-LDH is expected to be a new inorganic anion exchanger for the removal and recovery of nitrate ions from aquatic environments.

Keywords: bittern, ferric ion, layered double hydroxide, nitrate removal, synthesis

(Received 4 November 2020; revised 5 May 2021; Accepted Manuscript online: 14 May 2021; Associate Editor: Chun Hui Zhou)

Nitrate concentrations in water have increased in many agricultural areas during the past 10 years, mainly because of the use of the fertilizers as part of intensive agricultural production, one of the underlying reasons for artificial eutrophication. The development of an environmentally friendly and efficient technology to remove nitrate from contaminated water is becoming essential.

The need to ameliorate the toxicity of nitrates has created new technologies for nitrate removal from water (Canter, 1996), including physicochemical processes such as electrodialysis or reverse osmosis and biological processes using microorganisms to reduce nitrates into gaseous nitrogen. However, these processes are relatively expensive because of the equipment required, the production of large volumes of effluents and/or the long treatment times (Wan *et al.*, 2012). The adsorption method is good for the rapid, selective recovery of elements with markedly low concentrations. However, few adsorbents have been reported to facilitate the removal of nitrate ions from solutions that also contain large concentrations of chloride, sulfate or carbonate ions, because most of the adsorbents show low selectivity towards nitrate ions compared to other anions (Bhatnagar & Sillanpää, 2011; Lazaratou *et al.*, 2020).

Layered double hydroxides (LDHs) are layered minerals that have attracted much attention in recent years (Cavani *et al.*, 1991). The LDHs comprise positively charged layers with at least two different metal cations and negatively charged exchangeable interlayer anions. The general structural formula of LDHs can be expressed as $[M^{2+}_{1-x}M^{3+}_x(OH)_2]^{x+}(A^{n-})_{x/n}\cdot mH_2O$, where M^{2+} are divalent cations with similar ionic radii to Mg^{2+}, M^{3+} are trivalent cations with similar ionic radii to Al^{3+}, x is the $M^{2+}/(M^{2+}+M^{3+})$ ratio and A^{n-} is the exchangeable interlayer anion of valence n. Furthermore, ternary, quaternary or multivariate LDHs can be synthesized when a variety of metals is introduced into the layer to improve properties such as adsorption, catalysis and so on (Wang & O'Hare, 2012; Sun *et al.*, 2013; Gao *et al.*, 2014; Yang *et al.*, 2014; Kühl *et al.*, 2015). The properties of LDHs, namely their low cost, two-dimensional structure, large specific surface area, positive surface charge and large anion-exchange capacity, make them appropriate for a wide range of applications such as slow-release fertilizers (Gillman *et al.*, 2008), catalysts (Brito *et al.*, 2009; Zhou *et al.*, 2011; Lv *et al.*, 2015), nanosheets (Mao *et al.*, 2017) and flame retardants (Shi *et al.*, 2005), along with applications in the biomedical sector (Ren *et al.*, 2001; Wang & Zhang, 2012; Wang *et al.*, 2012; Li *et al.*, 2013) and in polymer nanocomposite synthesis (Costa *et al.*, 2008). Moreover, researchers are interested in using inexpensive precursors such as wastes and by-products instead of chemical salts for preparing a variety of target products, such as LDH materials. Such LDH products can be synthesized from iron-making slag (Wajima *et al.*, 2011, 2012; Kuwahara *et al.*, 2016; Wang *et al.*, 2016), aluminium dross (Murayama *et al.*, 2012), aluminium saline slag (Sntamaría *et al.*, 2020), red mud (Hu *et al.*, 2017), asbestos-containing waste (Li, 2019), biomass

*E-mail: wajima@tu.chiba-u.ac.jp
This paper was submitted for the special issue: 'Clays and Functional Materials' and was presented at the Asian Clay Conference, Singapore, 2020.
Cite this article: Wajima T (2021). Synthesis of Fe-layered double hydroxide from bittern and its nitrate-ion removal ability. *Clay Minerals* **56**, 65–74. https://doi.org/10.1180/clm.2021.17

© The Author(s), 2021. Published by Cambridge University Press on behalf of The Mineralogical Society of Great Britain and Ireland

https://doi.org/10.1180/clm.2021.17 Published online by Cambridge University Press

combustion ash (Suhara & Wajima, 2018), waste serpentine tailing (Zhu *et al.*, 2016), eggshell waste (Foruzin *et al.*, 2020) and bittern (Wajima, 2015).

Extensive previous work on nitrate removal using LDHs has been done by many authors (Socías-Viciana *et al.*, 2008; Terry, 2009; Islam & Patel, 2010, 2011; Wan *et al.*, 2012; Ivánová *et al.*, 2018). Among the LDH products, Fe-layered double hydroxide (Fe-LDH) has been reported to have selective nitrate removal ability (Tezuka *et al.*, 2004), and there are many studies on efficient nitrate removal using Mg-Fe-LDH (Sasai *et al.*, 2012; Yang *et al.*, 2015; Xue *et al.*, 2016; Tong *et al.*, 2017; Kamimoto *et al.*, 2019; Santos *et al.*, 2020). In our previous study, a Ca-Mg-Fe-LDH with nitrate-removal ability was synthesized from bittern with the addition of $FeCl_3$ (Wajima, 2018). Bittern is a by-product of the salt-refinement process, and it contains several ions (Mg^{2+}, Ca^{2+}, K^+ and Na^+) in greater concentrations than in seawater. This is especially the case for Mg and Ca ions, which are the most abundant cation species in bittern. Japan is an island nation which promotes the use of marine resources. Bittern is an important resource for application in various fields, and a novel LDH product synthesized from bittern may be used in new applications. LLimited information is available on the synthesis of Fe-LDH from bittern and its nitrate-removal ability.

There have been previous studies of nitrate removal using uncalcined LDH (Islam & Patel, 2009) and calcined LDH (Hosni & Srasra, 2007; Socias-Viciana *et al.*, 2008; Tong *et al.*, 2017) from model water. The hydrotalcite structure becomes disordered after thermal decomposition at 450–500°C, creating highly active mixed-metal oxides. The calcined products exhibited greater oxyanion adsorption efficiency than their uncalcined counterparts due to their significant thermal stability, increased specific surface area and porosity and fewer carbonate anions in the interlayer. The various mechanisms of anion adsorption of the calcined LDH in comparison with the uncalcined LDH are related to the reconstruction capability of the original laminar structure (known as the memory effect) *via* rehydration and the incorporation of various anions in the interlayers from aqueous solutions (Goh *et al.*, 2008). Calcined LDHs are not suitable for repeated use because regeneration of the calcined LDH necessitates calcination at a high temperature, which increases total costs. The present study focused, therefore, on uncalcined LDH as a reusable adsorbent for nitrate removal *via* the ion-exchange reaction.

In this study, we attempted to prepare an LDH adsorbent from bittern with good nitrate-removal performance. The product including Fe-LDH was prepared from bittern *via* the addition of an inexpensive agent ($FeCl_3$), and the nitrate-removal performance of the product was examined in various aqueous solutions. Synthesis of Fe-LDH from bittern by-products, control of the nitrate removal of the LDH product from bittern and the properties of the LDH regarding nitrate removal were analysed.

Experimental

Bittern and seawater

Commercial bittern was used to synthesize Fe-LDH, and seawater collected from the surface layer of Imari Bay, Saga Prefecture, Japan, was treated for the selective removal of nitrate. Table 1 lists the chemical compositions of the bittern and the seawater. The concentrations of the main elements in bittern were greater than those in seawater, except for SO_4^{2-}. The concentrations of Mg^{2+} and Ca^{2+} in bittern were 5432 and 1385 mmol L^{-1}, respectively. The seawater used in the experiment demonstrated the typical chemical composition of seawater. The pH values of bittern and the seawater were 5.4 and 7.8, respectively.

Table 1. Chemical composition (mmol L^{-1}) of bittern and the seawater.

	Na^+	K^+	Mg^{2+}	Ca^{2+}	Cl^-	SO_4^{2-}
Bittern	1591	926	5432	1385	16979	–
Seawater	422	10	53	10	522	46

Synthesis of Fe-LDH

The synthesis procedure of Fe-LDH from bittern is as follows (Fig. 1): $FeCl_3{\cdot}6H_2O$ (Wako) was added to 100 mL of bittern and stirred at room temperature (15–20°C) to prepare a mixed solution of $(Mg^{2+} + Ca^{2+})/Fe^{3+}$ (molar ratio of 3). A total of 100 mL of 1 mol L^{-1} NaCl solution was stirred at 20–80°C and the mixed solution was dropped into the NaCl solution at a rate of 4 mL min^{-1}. During stirring, the pH of the NaCl solution was maintained at 8.5–12.5 with 4 M NaOH. Additionally, N_2 gas was bubbled into the solution to inhibit the dissolution of carbon dioxide from the atmosphere. After 6 h of stirring, the precipitates were filtered, washed with distilled water and then dried at 60°C to obtain the product. The weights of the product were measured with an electric scale; furthermore, the mineralogical phases in the products were identified using X-ray diffraction (XRD; Miniflex600, Rigaku) with Cu-*Kα* radiation (30 kV, 15 mA) in the 2θ range of 5–55° with a scanning step of 0.02° and a speed of 5° min^{-1} and with a receiving Soller slit of 5°. The chemical composition of the product was determined by dissolving 50 mg of the LDH in 10 mL of 0.1 M HNO_3 solution, and determination of the Mg^{2+}, Ca^{2+} and Fe^{3+} contents was achieving using atomic absorption spectrometry (AAS; AAnalyst 2000, PerkinElmer).

Nitrate removal

To facilitate nitrate adsorption by the Fe-LDH, 50 mg of the product was added to a test tube containing 40 mL of 1 mmol L^{-1} $NaNO_3$ solution. The mixture was shaken for 30 min and subsequently centrifuged. The NO_3^- content in the supernatant was measured using the Cu–Cd reduction–*N*-(1-naphthyl)-ethylenediamine absorption method to calculate the NO_3^- removal rate (R) with Equation 1:

$$R = \frac{(C_0 - C)}{C_0} \times 100 \quad (1)$$

where C_0 and C are the initial and final concentrations of NO_3^- in the supernatant, respectively.

The nitrate removal reactions of the product were determined as follows: 500 mg of the product was added to 500 mL of 1 mmol L^{-1} $NaNO_3$ solution and the slurry was stirred with a magnetic stirrer for 6 h at 10–80°C. The pH of the solution was recorded during stirring with a pH meter (C-73, As One); aliquots of 4 mL were separated and filtered with a 20 μm membrane filter. The concentrations of NO_3^- were measured using the Cu–Cd reduction–*N*-(1-naphthyl)-ethylenediamine absorption method. The concentrations of Mg^{2+}, Ca^{2+} and Fe^{3+} eluted from the Fe-LDH into the solution were used to determine the elution amount

https://doi.org/10.1180/clm.2021.17 Published online by Cambridge University Press

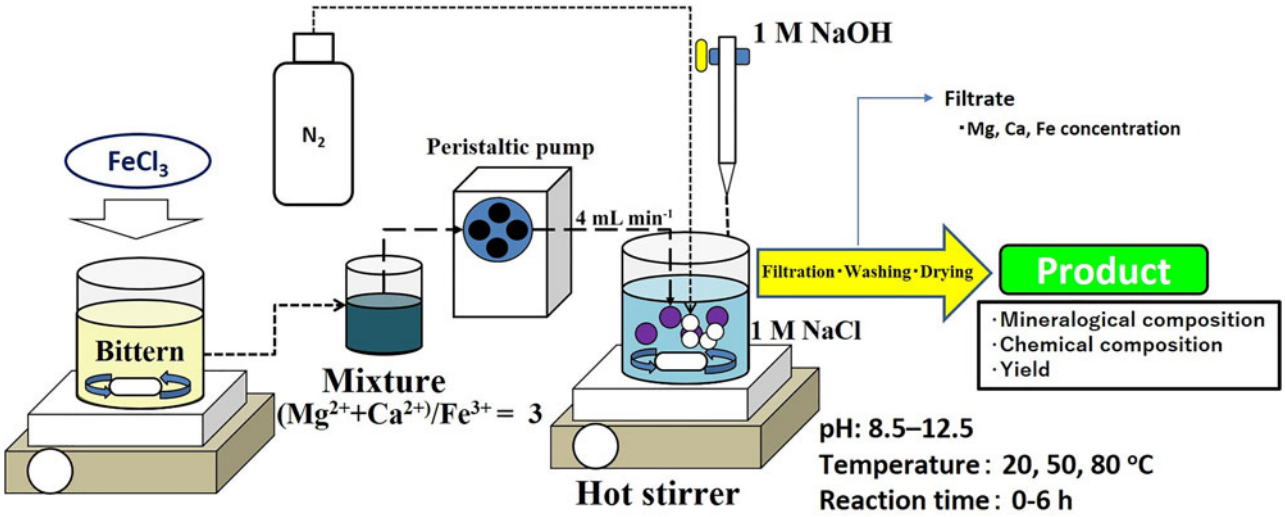


Fig. 1. Synthesis procedure of the Fe-LDH.

(E) using Equation 2:

$$E = \frac{C \bullet V}{w} \quad (2)$$

where C is the concentration of the ions, V is the volume (L) and w is the mass of the sample (g).

In addition, the nitrate-removal capacity of the Fe-LDH from the salty solution was determined using a seawater sample that was diluted by 0 to 10,000-fold. Thereafter, $NaNO_3$ powder was added to obtain an NO_3^- concentration of 0.1 mmol L^{-1}. The Fe-LDH (50 mg) was added to 40 mL of these solutions in 50 mL test tubes and the mixtures were shaken for 3 h using a reciprocal shaker. Then, the solid phase was separated *via* centrifugation, and the nitrate concentration of the supernatant was determined using the Cu–Cd reduction–*N*-(1-naphthyl)-ethylenediamine absorption method to calculate the nitrate-removal rate (R).

Furthermore, the effects of the coexisting anions on the nitrate-removal reactions of the product were determined as follows: 0.5 g of the product was added to 500 mL of 1 mmol L^{-1} $NaNO_3$ solution with 1 mmol L^{-1} NaCl, $NaNO_2$, Na_2SO_4, Na_2CO_3, NaBr and NaF, and the slurry was stirred magnetically for 6 h at room temperature. During stirring, the pH of the solution was measured with a pH meter; aliquots of 4 mL were separated, and a 20 μm membrane filter was used to obtain the filtrate. The nitrate concentration in the filtrate was measured using the Cu–Cd reduction–*N*-(1-naphthyl)-ethylenediamine absorption method.

To construct the nitrate adsorption isotherm, 50 mg of the product was added to 40 mL of 0.02–1.00 mmol L^{-1} $NaNO_3$ solution in test tubes and shaken for 20 min. The suspensions were then centrifuged and the nitrate content in the supernatant was measured using the Cu–Cd reduction–*N*-(1-naphthyl)-ethylenediamine absorption method to calculate the adsorption amount (q_e) with Equation 3:

$$q_e = \frac{(C_0 - C) \bullet V}{w} \quad (3)$$

To study the stability of nitrate ions on the Fe-LDH, adsorption and desorption cycles of nitrate ions were performed using 1 mM $NaNO_3$ as the absorbate and 5 mM NaCl as the eluent. The Fe-LDH (0.1 g) was added to 40 mL of 1 mM $NaNO_3$ solution in a 50 mL centrifuge tube, shaken for 10 min to adsorb nitrate ions and centrifuged to collect the supernatant. Then, 40 mL of 5 mM NaCl solution was added and the mixture was shaken for 10 min to desorb nitrate ions from the Fe-LDH, and this was then centrifuged. After removal of the supernatant, 40 mL of 1 mM $NaNO_3$ solution was added to the test tube again to adsorb the nitrate ions. This adsorption–desorption step was repeated ten times. The nitrate concentration in the supernatant was measured using the Cu–Cd reduction–*N*-(1-naphthyl)-ethylenediamine absorption method as per Equations 2 and 3.

Results and discussion

Preparation of Fe-LDH for nitrate removal

Figure 2a shows the XRD traces of the LDH synthesized in solutions with various pH values. The XRD traces of the products synthesized at pH 8.5–12.5 have symmetric peaks characteristic of hydrotalcite-like compounds (Ma *et al.*, 2017). The intensity of the 003 and 006 basal reflections decreased with a decrease in the pH of the synthesis solution, indicating a relatively well-formed crystalline Mg-LDH (Lv *et al.*, 2012).

The chemical compositions of the products synthesized in the solution at various pH values are listed in Table 2. A reduction in the pH value of the synthesis solution increased the Mg and Fe contents and decreased the Ca content; consequently, the (Mg + Ca)/Fe molar ratio and the yield of the LDH decreased. Thus, it is considered that Mg-Fe-LDH was synthesized at a lower pH, whereas Mg-Ca-Fe-LDH was synthesized at a higher pH.

The concentrations of Mg^{2+}, Ca^{2+} and Fe^{3+} in the synthesis solution are shown in Fig. 2b. By decreasing the pH of the synthesis solution, the Ca concentration increased after synthesis. Although the concentration of Mg was zero at pH 9.5–12.5, it was 35 mmol L^{-1} at pH 8.5. Moreover, the Fe content in the solution was zero regardless of the pH value, indicating that Fe was present entirely in the solid product after synthesis. Thus, the composition and yield of the products depended on the solubility of Ca in the synthesis solution at various pH values.

https://doi.org/10.1180/clm.2021.17 Published online by Cambridge University Press

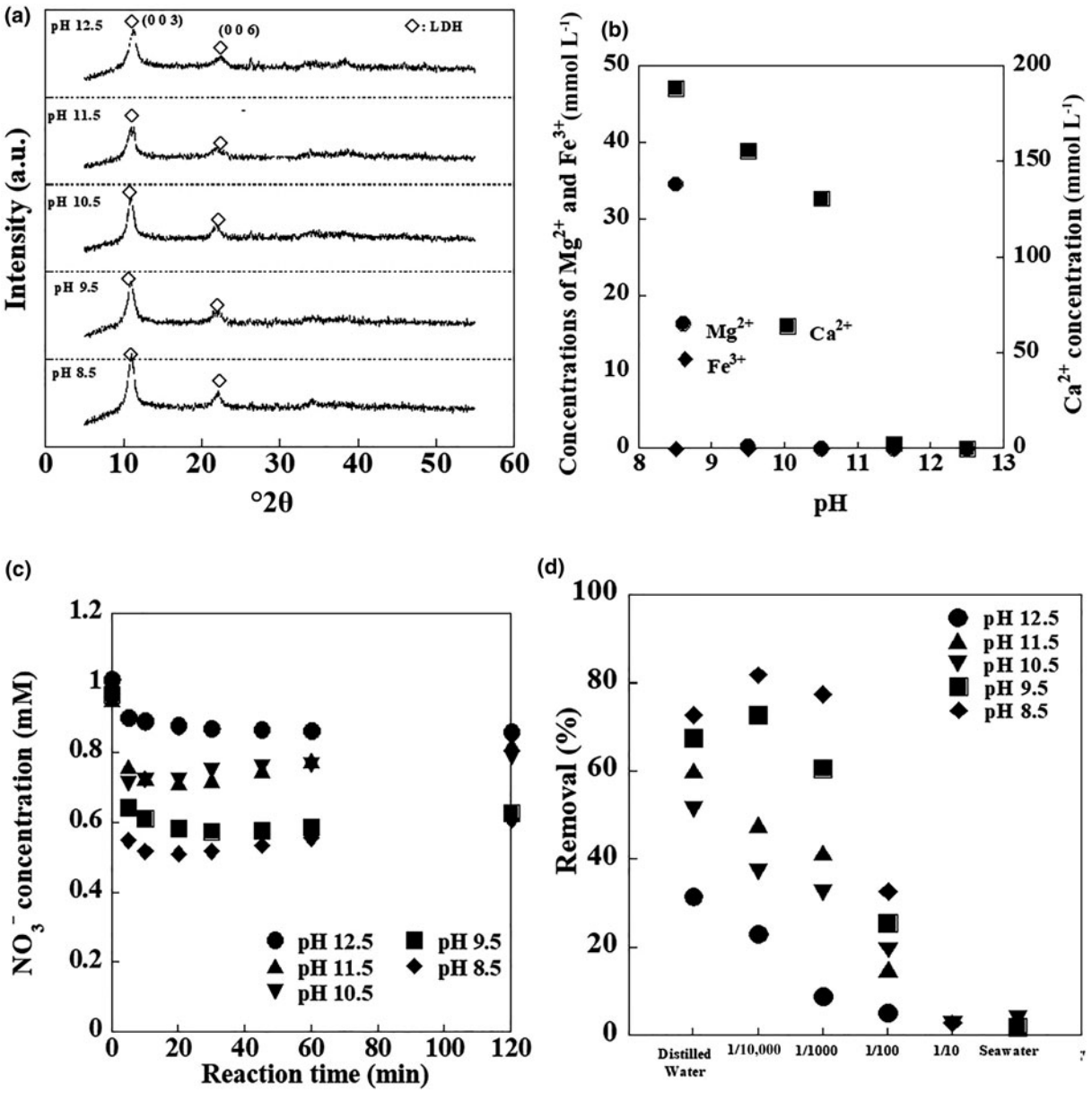


Fig. 2. (a) XRD traces of the products synthesized at pH 8.5–12.5. (b) Concentrations of Mg^{2+}, Ca^{2+} and Fe^{3+} in the solution after synthesis at pH 8.5–12.5. (c) NO_3^- concentration in the solution using the LDH product synthesized at pH 8.5–12.5. (d) NO_3^- removal in the saline solution using the LDH product synthesized at pH 8.5–12.5.

Table 2. Chemical composition of the Fe-LDH products synthesized from solution at various pH values.

	Contents (mmol g^{-1})				
pH	Mg	Ca	Fe	(Mg + Ca)/Fe	Yield (g)
12.5	6.93	1.97	2.47	3.60	37.2
11.5	6.73	1.95	2.57	3.38	37.6
10.5	7.60	0.82	2.87	2.93	34.9
9.5	8.65	0.54	3.10	2.97	32.2
8.5	7.63	0.32	3.12	2.55	30.8

The concentration of NO_3^- in the liquid after adsorption on LDH synthesized at pH 8.5–12.5 and 20°C decreased within 10 min, remaining almost constant thereafter (Fig. 2c). The products synthesized at a lower pH removed greater amounts of NO_3^- from the solution, and the NO_3^- concentration after 10 min of using the products synthesized at pH 8.5–9.5 yielded the lowest NO_3^- concentration of ~0.6 mmol L^{-1}. The solution pH was 10 and the elution of Mg^{2+}, Ca^{2+} and Fe^{3+} was <0.4 mmol g^{-1} after 20 min of reaction, regardless of the type of LDH. It is suggested that the crystal structure of the LDH synthesized at a greater pH might be partly destroyed by the increasing Ca^{2+} entering the brucite-like sheet, which decreased the nitrate-removal ability.

The nitrate removal from saline water by the LDH products is shown in Fig. 2d. The nitrate removal rate of products synthesized at pH 10.5–12.5 from seawater gradually decreased to 3% with increasing salinity. The nitrate removal rate of the LDH products synthesized at pH 8.5–9.5 was 60–80% in distilled water, 1/10,000

https://doi.org/10.1180/clm.2021.17 Published online by Cambridge University Press

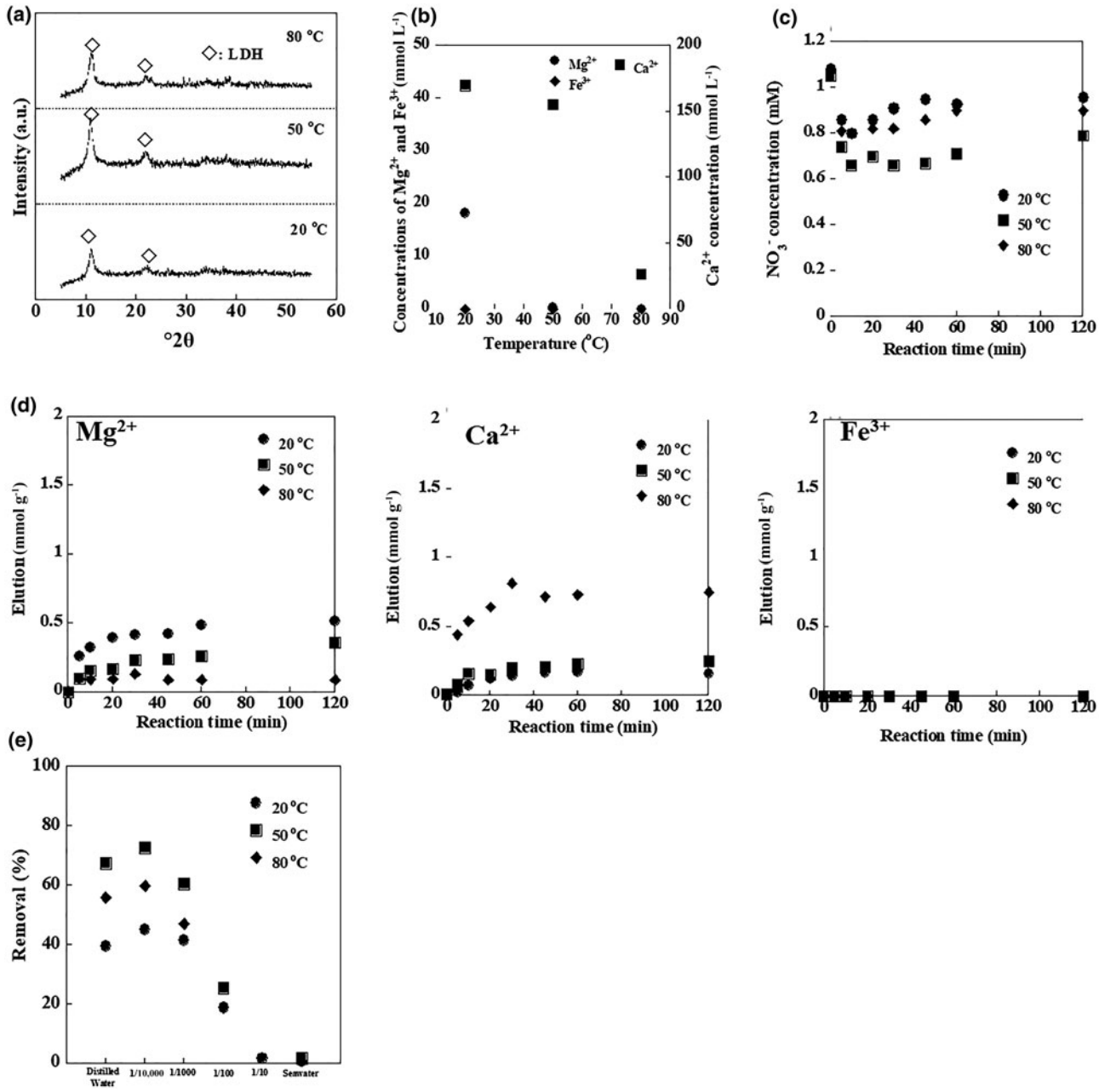


Fig. 3. (a) XRD traces of the LDH products synthesized at 20–80°C. (b) Concentrations of Mg^{2+}, Ca^{2+} and Fe^{3+} in the solution after synthesis at 20–80°C. (c) NO_3^- concentration in the solution using the product synthesized at 20–80°C. (d) Elution of Mg^{2+}, Ca^{2+} and Fe^{3+} in the NO_3^- solution from the LDH product synthesized at 20–80°C. (e) NO_3^- removal in the saline solution using the LDH product synthesized at 20–80°C.

seawater and 1/1000 seawater (freshwater environment), which is greater than those of the products at pH 10.5–12.5 owing to the greater nitrate-removal ability of Mg-Fe-LDH compared to Ca-Mg-Fe-LDH from saline water. Hence, the LDH synthesized at pH 8.5–9.5 exhibited greater removal ability for NO_3^- than those synthesized at pH > 10.5.

Figure 3a shows the XRD traces of the LDH synthesized at various temperatures and pH 9.5. The products contain hydrotalcite-like phases, and the crystal structure of the LDH synthesized at 80°C was partly destroyed by the incorporation of Ca^{2+} ions in the brucite-like sheet, which decreased the intensity of the 003 and 006 basal reflections. The product synthesized at 50°C showed the most intense LDH peaks.

Table 3. Chemical composition of the LDH products synthesized from solution at various temperatures.

	Contents (mmol g^{-1})				
Temperature (°C)	Mg	Ca	Fe	(Mg + Ca)/Fe	Yield (g)
20	7.89	0.51	3.05	2.75	32.3
50	8.66	0.54	3.10	2.97	32.2
80	7.58	1.60	2.59	3.54	36.7

The chemical compositions of the LDH end products synthesized at various temperatures are shown in Table 3. The Mg content of the product synthesized at 50°C was greater than that at

https://doi.org/10.1180/clm.2021.17 Published online by Cambridge University Press

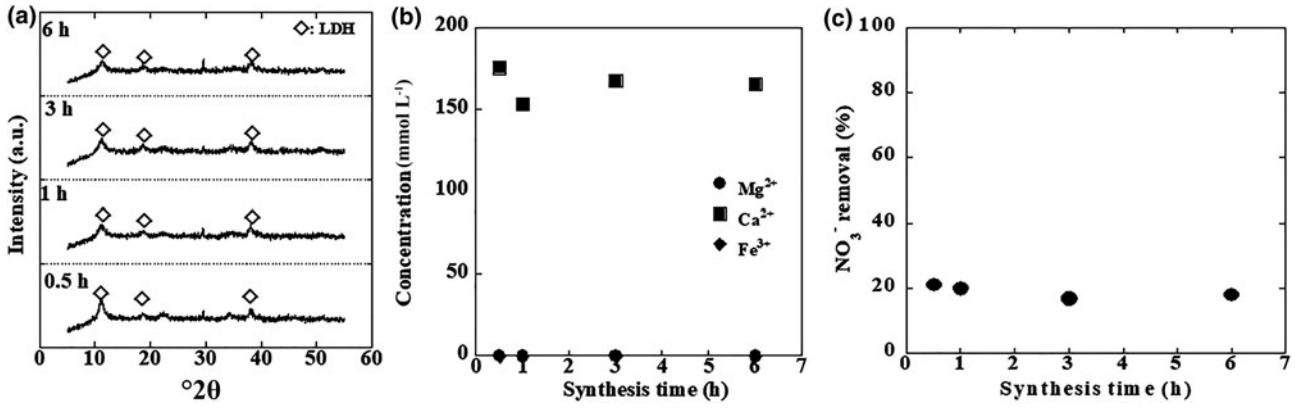


Fig. 4. (a) XRD traces of the LDH products synthesized for 0–6 h. (b) Concentrations of Mg^{2+}, Ca^{2+} and Fe^{3+} in the solution after synthesis for 0–6 h. (c) NO_3^- removal from the solution using the LDH product synthesized for 0–6 h.

20°C, whereas the Ca and Fe contents were almost the same, resulting in a greater (Mg + Ca)/Fe molar ratio of the product synthesized at 50°C. Moreover, the yield of the product at 50°C was almost identical to that at 20°C. In addition, the product synthesized at 80°C contained more Mg and Ca but less Fe than those synthesized at 20°C and 50°C, thus resulting in a greater (Mg + Ca)/Fe molar ratio of the product at 80°C. Therefore, the yield of the products was greater at 80°C than at 20°C or 50°C.

The concentrations of Mg^{2+}, Ca^{2+} and Fe^{3+} in the solution after synthesis are shown in Fig. 3b. Regardless of the synthesis temperature, the solution was Fe-free, indicating that Fe was hosted in the solid product after synthesis. The concentrations of Mg and Ca were 20 and 170 mmol L^{-1}, respectively, in the solution after synthesis at 20°C. With increasing synthesis temperature, the concentration of Ca remained almost constant, and the concentration of Mg reduced to zero in the solution at 50°C. At 80°C, the solution was free of Mg, and the Ca content decreased to 30 mmol L^{-1}. These results were in good agreement with the composition of the solids (Table 3).

The NO_3^- concentration in the solution after adsorption on the LDH products synthesized at 20–80°C is shown in Fig. 3c and the elution of Mg^{2+}, Ca^{2+} and Fe^{3+} from the LDH products into the NO_3^- solution is shown in Fig. 3d. The NO_3^- concentration in solution decreased within 10 min, remaining almost constant thereafter. The LDH product synthesized at 50°C removed a greater amount of NO_3^- from the solution, and the corresponding NO_3^- concentration after the 10 min treatment was minimal (~0.6 mmol L^{-1}). The NO_3^- concentration using the products at 20°C and 80°C was lower within the first 10 min but gradually increased at longer durations. The elution of Fe^{3+} from the products into the solution was negligible regardless of the synthesis temperature. The elution of Mg^{2+} and Ca^{2+} increased within 20 min of treatment and remained almost constant thereafter; the elution of Mg^{2+} from the LDH product synthesized at 20°C was greater than that of Ca^{2+} from the LDH product synthesized at 80°C. The increase in NO_3^- concentration in the solution after 10 min of treatment with products synthesized at 20°C and 80°C was due to the destruction of the LDH structure owing to the lower crystal order of the products synthesized at 20°C and 80°C compared to their counterparts synthesized at 50°C. After 20 min of reaction, the pH of the solution was alkaline (pH 10), regardless of the LDH products.

The removal of NO_3^- from saline water is shown in Fig. 3e. The nitrate removal rate of each LDH product remained almost constant upon increase of salinity of the solution to 1/1000 seawater and gradually decreased to 3% in seawater. The nitrate-removal rate of the LDH product synthesized at 50°C is 60–80% in distilled water, 1/10,000 seawater and 1/1000 seawater (freshwater environment), which is greater than that of the LDH product synthesized at 20°C (40%) and 80°C (50–60%); however, the removal rate decreased to 3% in seawater owing to the large amount of Mg-Fe-LDH in the solids. These results further confirmed that the LDH product synthesized at 50°C exhibited a greater removal ability for NO_3^- than the products synthesized at 20°C and 80°C.

Figure 4a shows the XRD traces of the LDH products synthesized in the solution for various times at pH 9.5 and 50°C, and the respective chemical compositions are shown in Table 4. The products contained hydrotalcite-like phases after 0.5 h of synthesis, and the chemical compositions and yields of the products were almost the same as in the remaining synthesis experiments. The concentrations of Mg^{2+}, Ca^{2+} and Fe^{3+} in the solution after synthesis are shown in Fig. 4b. Regardless of the synthesis period, the amounts of Ca^{2+} and Fe^{3+} in the solution were zero, and that of Mg was almost constant. Nitrate removal from the solution using the LDH products synthesized for 0–6 h is shown in Fig. 4c. Regardless of the synthesis period, the NO_3^- -removal capacities of the products were almost the same; thus, most NO_3^- was removed after a synthesis time of 0.5 h. Hence, the Fe-LDH product that was most effective for nitrate removal was synthesized in a solution with pH 9.5 at 50°C after 0.5 h.

Nitrate-removal ability

Figure 5 depicts nitrate removal from solution with various initial nitrate concentrations using the Fe-LDH product synthesized at pH 9.5 and 50°C for 0.5 h. The nitrate-removal rate decreased from 60% to 30% upon increasing the initial NO_3^- concentration from 0.05 to 1.0 mmol L^{-1}.

The isotherm of NO_3^- removal using the Fe-LDH product is shown in Fig. 6. The adsorption of NO_3^- increased with increasing equilibrium concentration. The adsorption isotherms were fitted with the Langmuir and Freundlich isotherm models. The linear forms of the Langmuir and Freundlich models are given by

https://doi.org/10.1180/clm.2021.17 Published online by Cambridge University Press

Table 4. Chemical composition of the LDH products synthesized from solution at various reaction times.

	Contents (mmol g^{-1})				
Synthesis time (h)	Mg	Ca	Fe	(Mg + Ca)/Fe	Yield (g)
0.5	8.28	0.74	3.19	2.82	30.9
1.0	8.28	0.64	3.10	2.88	30.9
3.0	8.15	0.70	3.02	2.93	31.3
6.0	8.31	0.57	3.04	2.93	31.1

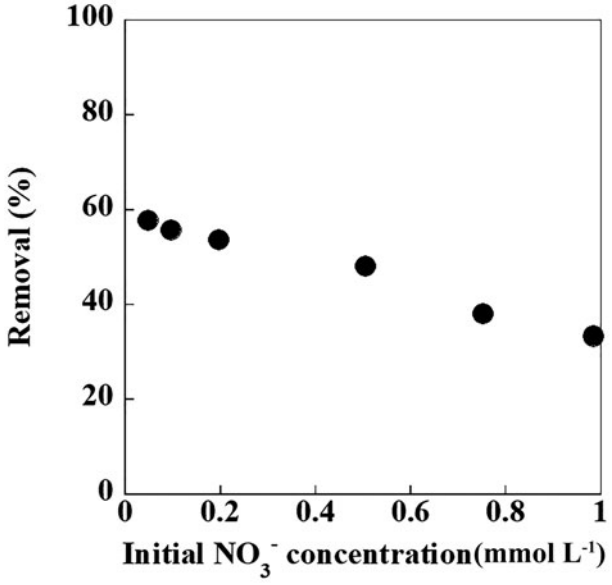


Fig. 5. Removal of NO_3^- from the solution with various initial NO_3^- concentrations.

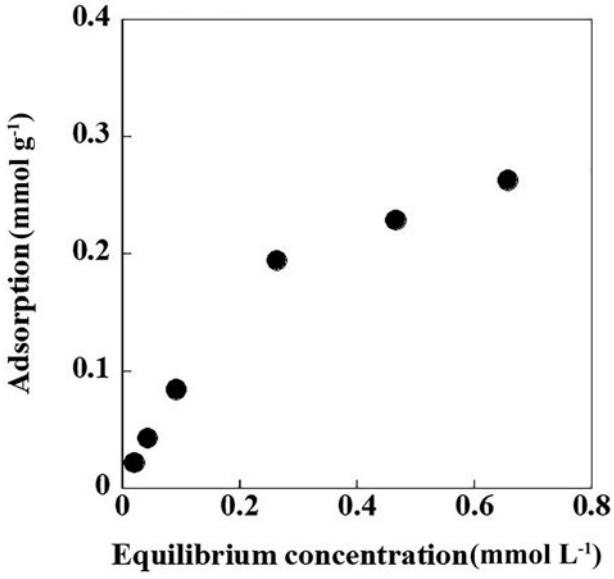


Fig. 6. Adsorption isotherm of NO_3^- on the Fe-LDH product.

Table 5. Langmuir and Freundlich parameters used to fit the NO_3^- adsorption isotherm.

Langmuir			Freundlich		
q_{max}	K_L	R^2	n	K_F	R^2
0.40	2.96	0.988	1.38	0.42	0.980

Table 6. Comparison of adsorption capacities of the LDH products for NO_3^- removal with previous work.

Adsorbent	Maximum adsorption capacity (mmol g^{-1})	Reference
Surfactant-modified clay minerals	0.24	Xi *et al.* (2010)
Bamboo biochars	0.08	Viglašová *et al.* (2018)
Onion peel dust	0.10	Mondal *et al.* (2019)
Activated carbon from babassu coconut	0.16	Paixão *et al.* (2018)
Activated carbon from sugar beet bagasse	0.15	Demiral & Gündüzoğlu (2010)
Mg-Fe-Cl-LDH	0.29	Santos *et al.* (2020)

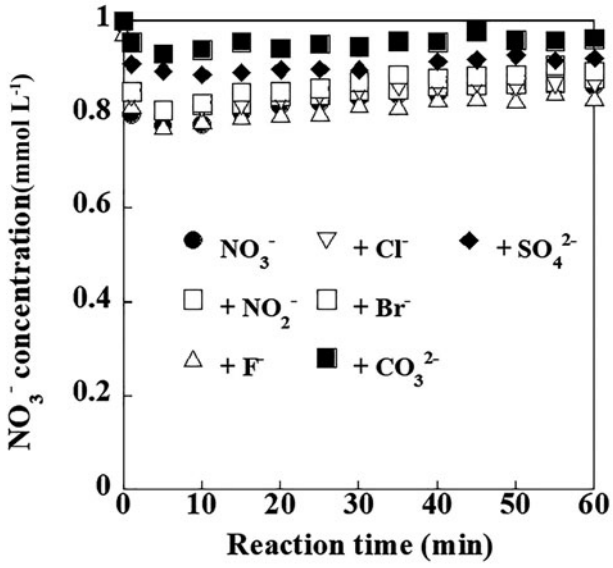


Fig. 7. NO_3^- concentration in the solution during reaction with various coexisting anions after the addition of LDH products.

Equations 4 and 5, respectively.

$$\frac{C_e}{q_e} = \frac{1}{(q_{max}K_L)} + \frac{1}{q_{max}}C_e \quad (4)$$

$$\ln(q_e) = \ln(K_F) + \frac{1}{n}\ln(C_e) \quad (5)$$

where q_e is the amount of nitrate adsorbed at equilibrium (mmol g^{-1}) and q_{max} (mmol g^{-1}) and K_L (L $mmol^{-1}$) are Langmuir constants related to the maximum adsorption capacity corresponding to complete coverage of the available sorption sites and a measure

https://doi.org/10.1180/clm.2021.17 Published online by Cambridge University Press

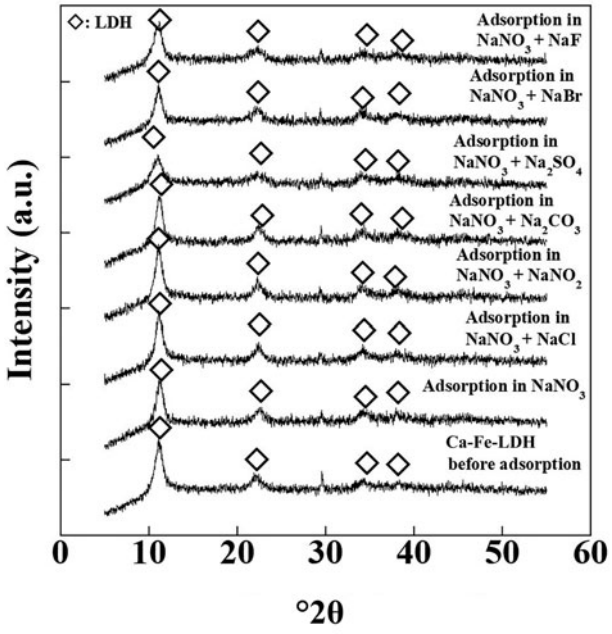


Fig. 8. XRD traces of the LDH products after the nitrate-removal test in solution with coexisting anions.

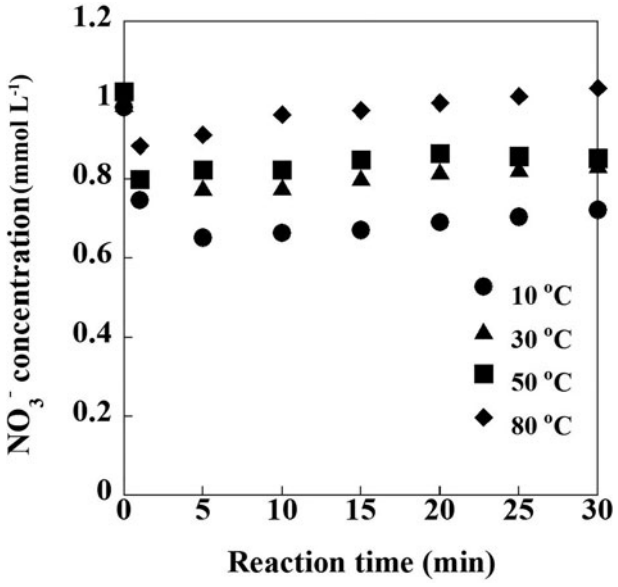


Fig. 9. NO_3^- concentration in the solution during reaction at various temperatures after the addition of LDH products.

of adsorption energy (equilibrium adsorption constant), respectively. K_F and n are the Freundlich constants.

The Langmuir and Freundlich constants and regression coefficients for NO_3^- removal are listed in Table 5. The coefficients of determination (R^2) indicate a better fit for the Langmuir model than the Freundlich model; the maximum adsorption capacity of the LDH product for NO_3^- calculated from the Langmuir model was 0.40 mmol g^{-1}. The adsorption capacity of the LDH product was greater than those of other adsorbents reported in previous studies (Table 6).

The NO_3^- concentrations in the solution during reaction with various coexisting anions are shown in Fig. 7. Regardless of the presence of anionic species, the NO_3^- concentrations in the solution decreased after 10 min of contact with the product, increasing gradually thereafter. The decrease of NO_3^- concentration in the solution containing monovalent anions was greater than that in solution with divalent anions because anions of greater valence are preferred over monovalent anions. For monovalent anions, the order of nitrate removal was $F^- > Cl^- > NO_2^- > Br^-$, because the greater ionic size (spherical diameter of F^-: 0.13 nm; Cl^-: 0.18 nm; Br^-: 0.20 nm; ellipsoids of NO_3^-: 0.29 nm × 0.15 nm; NO_2^-: 0.30 nm × 0.14 nm) affected the nitrate–ion exchange more. For divalent anions, the nitrate removal with SO_4^{2-} was preferred to that with CO_3^{2-}, which is similar to the results obtained using the biochar/Mg–Fe composite for nitrate removal, with the interfering effects of competing anions on nitrate adsorption following the order of $HCO_3^- > SO_4^{2-}$ (Xue *et al.*, 2016). The presence of carbonate reduced the nitrate adsorption on LDH. For example, the selectivity order for anion adsorption on Mg-Al-LDH exhibits the following magnitude relation of anion exchange reaction: carbonate > phosphate > sulfate > fluoride > chloride > bromide > nitrate (Miyata, 1983). The presence of competitive anions reduced the nitrate adsorption on Zn-Al-Cl-LDH as follows: carbonate > phosphate > chloride > sulfate (Islam & Patel, 2010). In this study, carbonate ions affected the adsorption of nitrate on LDH. Hence, carbonate contamination is an important limitation of nitrate adsorption on LDH. Therefore, it is necessary to remove carbonate anions by degassing with pressure reduction, ultrasound, etc., before water treatment with LDH.

The XRD traces of the LDH products after nitrate removal with various coexisting anions in the solution are shown in Fig. 8. The peaks of LDH were not affected by the coexisting anion species, indicating that the product removed NO_3^- from the solution through anion exchange without chemical precipitation of anions.

The NO_3^- concentrations in the solutions during the adsorption at various temperatures are shown in Fig. 9. The LDH products decreased rapidly the NO_3^- concentrations of solutions within 10 min, but the nitrate concentrations increased gradually over longer durations. The rate of nitrate removal from solutions decreased with decreasing temperature of solutions, indicating that the nitrate removal was an exothermic reaction. By contrast, nitrate removal using calcined Mg-Fe-LDH was an endothermic reaction (Yang *et al.*, 2015), the opposite of the anion-exchange reaction of nitrate using uncalcined Mg-Fe-LDH.

The XRD traces of the LDH products at various temperatures after nitrate removal are shown in Fig. 10. The peaks of LDH remained unchanged after nitrate removal at all temperatures, indicating that the product removed NO_3^- from the solution through ion exchange without affecting the LDH structure.

Figure 11 shows the adsorption capacity of the LDH products for nitrate ions after several adsorption/desorption cycles using 1 mM $NaNO_3$ and 5 mM NaCl solution. The amount adsorbed decreased from 0.28 to 0.09 mmol g^{-1}, remaining virtually constant at 0.09 mmol g^{-1} after six cycles. The amount desorbed increased from 0.14 to 0.18 mmol g^{-1} in the first three cycles, then decreased to 0.09 mmol g^{-1}, and finally remained almost constant at 0.09 mmol g^{-1} after six cycles. The percentage of nitrate desorption after adsorption was ~50% in the first cycle, exceeding 100% up to six cycles, and then being ~100%. The LDH product exhibited a constant capacity for nitrate-ion exchange after seven cycles when almost the same amount of nitrate ions were adsorbed and desorbed, thereby attaining

https://doi.org/10.1180/clm.2021.17 Published online by Cambridge University Press

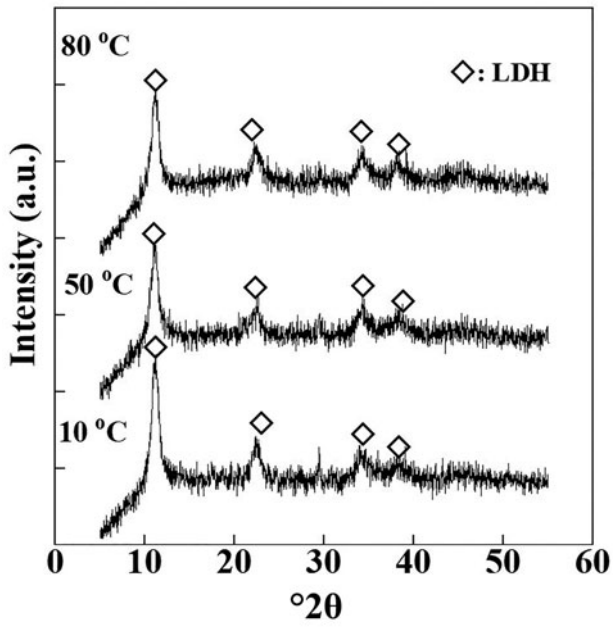


Fig. 10. XRD traces of the LDH products after nitrate removal at various temperatures.

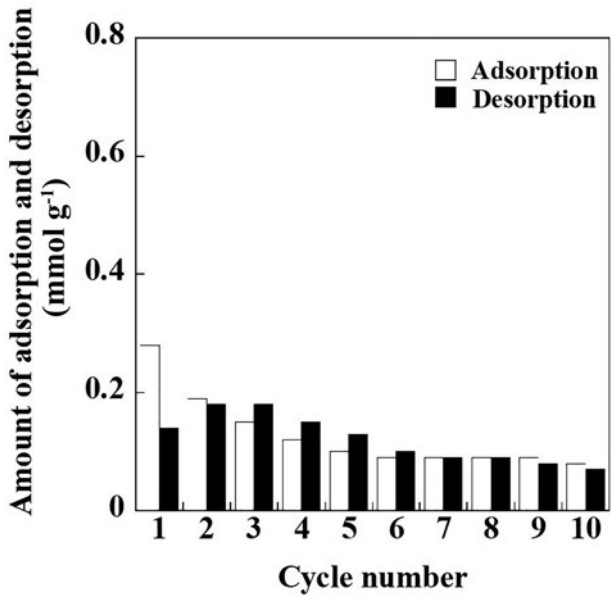


Fig. 11. Adsorption capacity of the LDH product for nitrate ions after repeated adsorption cycles. Adsorption was performed with 1 mM $NaNO_3$ solution and desorption was performed with 5 mM NaCl solution.

equilibrium between exchangeable Cl^- in LDH and NO_3^- in the solution. Hence, the LDH product may be used repeatedly to remove nitrate ions with NaCl solution as the eluent.

Conclusions

An Fe-LDH was synthesized from bittern with the addition of $FeCl_3$ for the removal of nitrate ions. The Fe-LDH product had the greatest nitrate-removal ability at synthesis conditions of pH 8.5–9.5, temperature 50°C and synthesis time 0.5 h. The LDH product removed nitrate ions from a highly saline solution, and the order of interference of anion species for nitrate removal was $CO_3^{2-} > SO_4^{2-} > Br^- > NO_2^- > Cl^- > F^-$. The solution pH and nitrate removal were greater with increasing solution temperature because of the ion exchange between Cl^- in Fe-LDH and NO_3^- in the solution. The product adsorbed and then desorbed nitrate ions in several cycles using NaCl solution. This work has demonstrated potential applications of the LDH product as a green absorbent for nitrate removal from water and as a soil amendment for the reduction of soil nitrate.

Financial support. This work was supported by the Salt Science Research Foundation, No. 1625.

References

Bhatnagar A. & Sillanpää M. (2011) A review of emerging adsorbents for nitrate removal from water. *Chemical Engineering Journal*, **168**, 493–504.

Brito A., Borges M.E., Garin M. & Hernandez A. (2009) Biodiesel production from waste oil using Mg–Al layered double hydroxide catalysts. *Energy & Fuels*, **23**, 2952–2958.

Canter L.W. (1996) *Nitrates in Groundwater*. CRC Press, Boca Raton, FL, USA, 288 pp.

Cavani F., Trifirò F. & Vaccari A. (1991) Hydrotalcite-type anionic clays: preparation, properties and applications. *Catalysis Today*, **11**, 173–301.

Costa F.R., Leuteritz A., Wagenknecht U., Jehnichen D., Häußler L. & Heinrich G. (2008) Intercalation of Mg–Al layered double hydroxide by anionic surfactants: preparation and characterization. *Applied Clay Science*, **38**, 153–164.

Demiral H. & Gündüzoğlu G. (2010) Removal of nitrate from aqueous solutions by activated carbon prepared from sugar beet bagasse. *Bioresource Technology*, **101**, 1675–1680.

Foruzin L.J., Rezvani Z. & Habibi B. (2020) New ternary-component layered double hydroxide as a low-cost and efficient electrocatalyst for water oxidation: NiCaFe-LDH from eggshell biowaste. *Applied Clay Science*, **188**, 105511.

Gao P., Li F., Zhan H.J., Zhao N., Xiao F., Wei W. *et al.* (2014) Fluorine-modified Cu/Zn/Al/Zr catalysts *via* hydrotalcite-like precursors for CO_2 hydrogenation to methanol. *Catalysis Communications*, **50**, 78–82.

Gillman G.P., Nobel M.A. & Raven M.D. (2008) Anion substitution of nitrate-saturated layered double hydroxide of Mg and Al. *Applied Clay Science*, **38**, 179–186.

Goh K.H., Lim T.T. & Dong Z. (2008) Application of layered double hydroxides for removal of oxyanions: a review. *Water Research*, **42**, 1342–1368.

Hosni K. & Srasra E. (2007) Nitrate adsorption from aqueous solution by M^{II}-Al-CO_3 layered double hydroxide. *Inorganic Materials*, **44**, 742–749.

Hu P., Zhang Y., Lv F., Tong W., Xin H., Meng Z. *et al.* (2017) Preparation of layered double hydroxides using boron mud and red mud industrial wastes and adsorption mechanism to phosphate. *Water and Environment Journal*, **31**, 145–157.

Islam M. & Patel R. (2009) Nitrate sorption by thermally activated Mg/Al chloride hydrotalcite-like compound. *Journal of Hazardous Materials*, **169**, 524–531.

Islam M. & Patel R. (2010) Synthesis and physicochemical characterization of Zn/Al chloride layered double hydroxide and evaluation of its nitrate removal efficiency. *Desalination*, **256**, 120–128.

Islam M. & Patel R. (2011) Physicochemical characterization and adsorption behaviour of Ca/Al chloride hydrotalcite-like compound towards removal of nitrate. *Journal of Hazardous Materials*, **190**, 659–668.

Ivánová D., Albert P. & Kavuličová J. (2018) Nitrate removal from model aqueous solutions and real water by calcined Mg/Al layered double hydroxides. *Applied Clay Science*, **152**, 65–72.

Kamimoto Y., Okamoto N., Hagio T., Yong-Jun J., Deevanhxay P. & Ichino R. (2019) Development of magnesium–iron layered double hydroxide and application to nitrate removal. *SN Applied Sciences*, **1**, 1399.

Kühl S., Schumann J., Kasatkin I., Hävecker M., Schlögl R. & Behrens M. (2015) Ternary and quaternary Cr or Ga-containing ex-LDH catalysts –

https://doi.org/10.1180/clm.2021.17 Published online by Cambridge University Press

influence of the additional oxides onto the microstructure and activity of $Cu/ZnAl_2O_4$ catalysts. *Catalysis Today*, **246**, 92–100.
Kuwahara Y., Tamagawa S., Fujitani T. & Yamashita H. (2016) Removal of phosphate from aqueous solution using layered double hydroxide prepared from waste iron-making slag. *Bulletin of Chemical Society of Japan*, **89**, 472–480.
Lazaratou C.V., Vayenas D.V. & Papoulis D. (2020) The role of clays, clay minerals and clay-based materials for nitrate removal from water systems: a review. *Applied Clay Science*, **185**, 105377.
Li S. (2019) Synthesis of layered double hydroxide from asbestos-containing waste and it adsorption property. *Journal of Material Cycles and Waste Management*, **21**, 1242–1249.
Li S., Li J., Wang C.J., Wang Q, Cader M.Z., Lu J. *et al*. (2013) Cellular uptake and gene delivery using layered double hydroxide nanoparticles. *Journal of Materials Chemistry*, **B1**, 61–68.
Lv W.M., Yang L., Fan B.B., Zhao Y., Chen Y.F., Lu N.Y. & Li R.F. (2015) Silylated MgAl LDHs intercalated with MnO_2 nanowires: highly efficient catalysts for the solvent-free aerobic oxidation of ethylbenzene. *Chemical Engineering Journal*, **263**, 309–316.
Lv T., Ma W., Xin G., Wang R., Xu J., Liu D. *et al*. (2012) Physicochemical characterization and sorption behavior of Mg-Ca-Al(NO_3) hydrotalcite-like compounds toward removal of fluoride from protein solutions. *Journal of Hazardous Materials*, **237–238**. 121–132.
Ma W., Chen Y., Zhang W. & Zhao W. (2017) Performance and mechanism of Mg–Ca–Fe hydrotalcite-like compounds for fluoride removal from aqueous solution. *Journal of Fluorine Chemistry*, **200**, 153–161.
Mao N., Zhou C.H., Tong D.S., Yu W.H. & Lin C.X.C. (2017) Exfoliation of layered double hydroxide solids into functional nanosheets. *Applied Clay Science*, **144**, 60–78.
Miyata S. (1983) Anion-exchange properties of hydrotalcite-like compounds. *Clays and Clay Minerals*, **31**, 305–311.
Mondal N.K., Ghosh P., Sen K., Mondal A. & Debnath P. (2019) Efficacy of onion peel toward removal of nitrate from aqueous solution and field samples. *Environmental Nanotechnology, Monitoring and Management*, **11**, 100222.
Murayama N., Maekawa I., Ushiro H. & Miyoshi T. (2012) Synthesis of various layered double hydroxides using aluminium dross generated in aluminium recycling process. *International Journal of Mineral Processing*, **110–111**, 46–52.
Paixão R.M., Reck I.M., Bergamasco R., Vieira M.F. & Vieira A.M.S. (2018) Activated carbon of babassu coconut impregnated with copper nanoparticles by green synthesis for the removal of nitrate in aqueous solution. *Environmental Technology*, **39**, 1994–2003.
Ren L., He J., Evans D.G., Duan X. & Ma R. (2001) Some factors affecting the immobilization of penicillin G acylase on calcined layered double hydroxides. *Journal of Molecular Catalysis B – Enzymatic*, **16**, 65–71.
Santamaria L., Lopez-Aizpun M., Garcia-Padial M., Vicente M.A., Korili S.A. & Gil A. (2020) Zn–Ti–Al layered double hydroxides synthesized from aluminium saline slag wastes as efficient drug adsorbents. *Applied Clay Science*, **187**, 105486.
Santos L.C., Silva A.F., Lins P.V.S., Duarte J.L.S., Ide A.H. & Meili L. (2020) Mg–Fe layered double hydroxide with chloride intercalated: synthesis, characterization and application for efficient nitrate removal. *Environmental Science and Pollution Research*, **27**, 5890–5900.
Sasai R., Norimatsu W. & Matsumoto Y. (2012) Nitrate-ion-selective exchange ability of layered double hydroxide consisting of Mg^{II} and Fe^{III}. *Journal of Hazardous Materials*, **215–216**, 311–314.
Shi L., Li D., Wang J., Li S., Evans D.G. & Duan X. (2005) Synthesis, flame-retardant and smoke-suppressant properties of a borate-intercalated layered double hydroxide. *Clay and Clay Minerals*, **53**, 294–300.
Socias-Viciana M.M., Urena-Amate M.D., Gonzáles-Prades E., Garcia-Cortés M.J. & López-Teruel C. (2008) Nitrate removal by calcined hydrotalcite-type compounds. *Clays and Clay Minerals*, **56**, 2–9.
Suhara A. & Wajima T. (2018) Synthesis of Fe-type layered double hydroxide from biomass combustion ash for removal of arsenite and arsenate. *Journal of Ion Exchange*, **29**, 60–66.
Sun Z., Lin C., Zheng J., Wang L., Zhang J., Xu F. & Hou J. (2013) Fabrication and characterization of hierarchical Mg/Ni/Al layered double hydroxide framework on aluminum foam. *Materials Letters*, **113**, 83–86.
Terry P.A. (2009) Removal of nitrates and phosphates by ion exchange with hydrotalcite. *Environmental Engineering Science*, **26**, 691–696.
Tezuka S., Chitrakar R., Sonoda A., Ooi K. & Tomida T. (2004) Studies on selective adsorbents for oxo-anions. Nitrate ion-exchange properties of layered double hydroxides with different metal atoms. *Green Chemistry*, **6**, 104–109.
Tong X., Yang Z., Xu P., Li Y. & Niu X. (2017) Nitrate adsorption from aqueous solutions by calcinated ternary Mg–Al–Fe hydrotalcite. *Water Science and Technology*, **75**, 2194–2203.
Viglašová E., Galamboš M., Danková Z., Krivosudský L., Lengauer C.L., Hood-Nowotny R. *et al*. (2018) Production, characterization and adsorption studies of bamboo-based biochar/montmorillonite composite for nitrate removal. *Waste Management*, **79**, 385–394.
Wajima T. (2015) Synthesis of hydrotalcite from bittern, and its removal abilities of phosphate and nitrate. *International Journal of Chemical Engineering and Applications*, **6**, 228–231.
Wajima T., Oya K., Shibayama A., Sugawara K. & Munakata K. (2011) Synthesis of hydrocalumite-like adsorbent from blast furnace slag using alkali fusion. *ISIJ International*, **51**, 1179–1184.
Wajima T., Oya K., Shibayama A. & Munakata K. (2012) Preparation of adsorbent with high removal ability for phosphate ion from blast furnace slag using alkali fusion. *International Journal of the Society of Materials Engineering for Resources*, **18**, 59–63.
Wan D.J., Liu H.J., Liu R.P., Qu J.H., Li S.S. & Zhang J. (2012) Adsorption of nitrate and nitrite from aqueous solution onto calcined (Mg–Al) hydrotalcite of different Mg/Al ratio. *Chemical Engineering Journal*, **195–196**, 241–247.
Wang Q. & O'Hare D. (2012) Recent advances in the synthesis and application of layered double hydroxide (LDH) nanosheets. *Chemical Reviews*, **112**, 4124–4155.
Wang Y. & Zhang D. (2012) Synthesis, characterization, and controlled release antibacterial behavior of antibiotic intercalated Mg–Al layered double hydroxides. *Materials Research Bulletin*, **47**, 3185–3194.
Wang Y., Zhang D., Bao Q., Wu J.J. & Wan Y. (2012) Controlled drug release characteristics and enhanced antibacterial effect of graphene oxide–drug intercalated layered double hydroxide hybrid films. *Journal of Materials Chemistry*, **22**, 23106–23113.
Wang C., Chen Y., Shang X., Hou X. & Li H. (2016) Facile synthesis of Ca/Mg/Al/Fe layered double hydroxides using steelmaking slag as raw material. *Materials Letters*, **173**, 115–118.
Xi Y., Mallavarapu M. & Naidu R. (2010) Preparation, characterization of surfactants modified clay minerals and nitrate adsorption. *Applied Clay Science*, **48**, 92–96.
Xue L., Gao B., Wan Y., Fang J., Wang S., Li Y. *et al*. (2016) High efficiency and selectivity of MgFe-LDH modified wheat-straw biochar in the removal of nitrate from aqueous solutions. *Journal of the Taiwan Institute of Chemical Engineers*, **63**, 312–317.
Yang R.Y., Gao Y.S. & Wang J.Y. (2014) Layered double hydroxide (LDH) derived catalysts for simultaneous catalytic removal of soot and NO_x. *Dalton Transactions*, **43**, 10317–10327.
Yang Z., Zhang L., Xu P., Zhang X., Niu X. & Zhou S. (2015) The adsorption of nitrate from aqueous solution onto calcined Mg/Fe hydrotalcite. *Desalination and Water Treatment*, **54**, 3400–3411.
Zhou C.H., Beltramini J.N., Lin C.X., Xu Z.P., Lu G.Q. & Tanksale A. (2011) Selective oxidation of biorenewable glycerol with molecular oxygen over Cu-containing layered double hydroxide-based catalysts. *Catalysis Science and Technology*, **1**, 111–122.
Zhou P., Li Z.L., Hao Y., Qian G.R. & Zhou J. (2016) Novel approach to synthetic Mg(II)Fe(III) layered double hydroxide using waste serpentine tailing. *Journal of Hazardous Toxic and Radioactive Waste*, **21**, 06016002.

https://doi.org/10.1180/clm.2021.17 Published online by Cambridge University Press